Journals Pub

International Journal of
Green Chemistry

ISSN: 2582-5925
Volume 11, Issue 1, 2025
DOI (Journal): 10.37628/IJGC

http://mechanical.journalspub.info/index.php?journal=IJMD&page=index

Research IJGC

Structure and Dynamics of Carbon Dangling Bonds in Activated Carbon Materials from Biomass

Indra Neel Pulidindi[1], Varadarajan Thirukallam Kanthadai[2], Viswanathan Balasubramanian[3,*]

Abstract

Activated carbon materials are inevitable for energy-related applications. Production of such materials from biomass is sustainable. Microporous activated carbon materials with high specific surface area and pore sizes of less than 2 nm find life-saving applications apart from their utility in environmental remediation. The free electron density of these materials is tunable and is a measure of the electrical conductivity useful for the development of green and renewable energy sources. A simple and economically viable methodology is reported for the sulfur functionalized nanoporous activated carbon material derived from wasteland weed native to India, namely, Ipomoea carnea. Owing to the presence of high spin concentration the material holds the promise of ideal adsorbent for environmental contaminants apart from being used as a potential electrode material for energy conversion as well as energy storage devices that operate on the principles of catalysis. The electrical conductivity in activated carbon materials is proportional to the free electron density. A successful attempt has been made to synthesize sulfur-functionalized activated carbon material from Ipomoea carnea, a representative wasteland weed native of India.

Keywords: Spin concentration, electrical conductivity, carbon materials, dangling bonds, biomass, *Ipomoea carnea*, EPR.

INTRODUCTION

The chemistry of producing porous carbon materials from biomass is more than a century old [1]. Credit is due to the Polish Chemist Rafal von Ostrejko whose inventions about activated carbon production from biomass saved many human lives during World War I [2–4]. Masks with activated carbon materials produced in the earliest factory built in Ratibor in the German empire (currently in Poland) were of immense use in saving human lives from chemical warfare agents. Currently, we are living in times no different from those of World War I (1914–1918). Such life-saving applications of activated carbon materials can be anticipated during these turbulent days of catastrophic climate change, resource depletion, and war as seen in Israel and Russia [5].

Catastrophic climate change events and worsening energy crises necessitate the invention of alternate green energy conversion and storage devices for the sustenance and development of human societies [6–13]. Fuel cells and supercapacitor batteries are some famous examples of such promising green energy storage devices that exhibit high energy density and power density and operate on carbon-based electrode materials [14]. Improvement in the performance of the electrochemical devices is dependent on the development of advanced electrode materials with

***Author for Correspondence**
Viswanathan Balasubramanian
E-mail: bviswanathan@gmail.com

[1]Research Consultant, Department of Chemistry, Jesus' Scientific Consultancy for Industrial and Academic Research (JSCIAR), Chennai, Tamil Nadu, India.
[2] Research Scientist, Department of Chemistry, Indian Institute of Technology, Chennai, Tamil Nadu, India.
[3]Retired Professor, Department of Chemistry, Indian Institute of Technology, Chennai, Tamil Nadu, India.

Received Date: January 01, 2025
Accepted Date: January 05, 2025
Published Date: January 10, 2025

Citation: Indra Neel Pulidindi, Varadarajan Thirukallam Kanthadai, Viswanathan Balasubramanian. Structure and Dynamics of Carbon Dangling Bonds in Activated Carbon Materials from Biomass Dedicated, in Fond Memory, to the Famous Surface Chemist Late Professor Alvin W. Czanderna Who Slept in the Lord on June 5, 2023. International Journal of Green Chemistry [IJGC]. 2025; 11(1): 18–27p.

high spin concentrations. Not only the concentration of the free electrons but also their geometric arrangement over the carbon surface is crucial for the device performance which is an untrodden area and grey region in the research about electrochemical energy sources. The preparation of high-performance carbon materials for electrode application is a challenge. There is an urgent need to develop high-performance carbon materials rich in free electron concentration in the desired geometrical orientation under mild process conditions from renewable resources reducing the environmental impact. Biomass is a potential precursor for carbon materials with unique microstructure and texture, porosity, and chemical and electrochemical properties. Other advantages of high-performance carbon materials from biomass include tunable porosity, high specific surface area, and a high degree of graphitization. Though there have been several studies on carbon materials from biomass, improvement in the properties of the material is still desired [14–20].

It is an innovative strategy to develop electrode materials based on carbon materials from biomass with desired free electron concentration. Such a strategy simultaneously alleviates the problems of energy and environmental crises. Moreover, carbon materials from biomass are unique and evolving. These materials have peculiar properties like high free electron (spin) concentration that render exceptionally high electrochemical potential for electrochemical device applications like fuel cells, supercapacitors, and batteries [21]. The present research paper is aimed at evaluating the tunability of free electron concentration of biomass mass-derived carbon material relative to activated carbon materials derived from fossil resources for improving the electrochemical performance (volumetric capacitance, energy density, power density cyclability, and rate characteristics) of electrochemical energy sources in general. The biomass that was employed in the study for producing activated carbon materials with high spin concentrated comprised of waste weeds (stems of *Calotropis gigantea* and *Ipomoea carnea*) as well as food wastes, namely, shells of *Limonea acidissima*) native to India as shown in Figure 1 [22].

Figure 1. Stems of *Calotropis gigantea* (gilledu) (a), *Ipomoea carnea* (thutu) (b), and shells of *Limonea acidissima* (velaga) (c). (Text in the brackets represents native terms of Indian origin).

Scrutiny of the existing literature by crossing the keywords namely, carbon materials and free electron concentration yielded only 1245 results from the Web of Science (under all fields, as of 10th July 2024). Such an in-depth study on the relationship between the free electron concentration of carbon materials and their electrochemical performance is a new avenue and forms a fertile research area though less investigated. The current study thus lays a foundation for such free electron concentration and performance relationship in carbon materials derived from biomass.

EXPERIMENTAL

Chemicals

Commercial activated carbon material, namely, Vulcan XC 72 R was purchased from Cabot Corporation, USA. Nuchar activated carbon was procured from Mead Westvaco chemical division, USA. Calgon Carbon was purchased from Calgon Carbon (Tianjin) Co. Ltd., China. Graphite fine powder is purchased from Loba Chemie Pvt. Ltd., India. Sulfur and hydrazine hydrate were procured from SD Fine Chem Ltd., India. All the chemicals and solvents used for the investigation were of analytical (AR) grade. The chemicals were used as such without further purification.

Preparation of Carbon Materials from *Ipomoea carnea* Stems

Systematic procedures adopted for the synthesis of biochar, its treatment with a base and an acid in succession, and its further functionalization with S were as follows. The biochar from the stems of *Ipomoea carnea* was prepared by taking the dried stems of *Ipomoea carnea* (22.434 g) and pyrolyzing them in an N_2 atmosphere at 400°C for 8 h. Devolatilization and subsequent carbonization took place. The yield of the carbon material as synthesized is 8.88 g (39.6%). The obtained biochar was subsequently treated with a base and an acid in succession. The biochar was treated with 43 mL of 10 wt.% NaOH solution for 1 h. The contents were then filtered through a 200 mL G4 sintered funnel. The yield of the base-treated carbon material is 3.636 g (84.5%). The loss in wt. after NaOH treatment is 0.664 g (15.4%) which corresponds to the impurities (SiO_2) soluble in NaOH. The base-treated carbon material (3.636 g) was subsequently treated with 36 mL of conc. HCl for 1 h. The contents are then filtered and washed with excess distilled water. The yield of the carbon material after acid treatment is 3.246 g (89.4 %). The weight loss of 0.39 g (10.7%) corresponds to the metal as well as other impurities soluble in conc. HCl. The carbon material from *Ipomoea carnea* thus obtained after base and acid treatment was functionalized with sulfur by a simple method where N_2 gas is bubbled through a solution of elemental sulfur dissolved in hydrazine monohydrate. The process of S functionalization is carried out in a tubular furnace at 400 °C in a quartz tube. 6.0 g of carbon material (base and acid treated) to be functionalized with S is taken in an alumina boat. The alumina boat with the carbon sample is placed in a tubular furnace. N_2 gas is bubbled through a solution of S (24.05 g) dissolved in hydrazine monohydrate (60.05 g) (the method of preparation of S solution in hydrazine is given below). The process of S functionalization is carried out for 4 h. The initial volume of the solution of S in hydrazine is 42 mL and the final volume after 4 h treatment of the carbon material is 32 mL implying that 10 mL of S in hydrazine monohydrate solution is consumed during the process of impregnation. The yield of the S-impregnated carbon material is 4.567 g (76 %). Thus, the activated carbon material from *Ipomoea carnea* functionalized with S is obtained**.** Since the reaction between hydrazine and sulfur is exothermic, the reaction is carried out under ice-cold conditions. Hydrazine hydrate (60.05 g, 58.47 mL, d = 1.027 g/mL, Mol. Wt. = 50.06 g) is taken in a beaker placed in a trough with ice cubes. A magnetic pellet is placed in the beaker. The contents in the beaker are subjected to stirring. Sulfur (24.05 g, Mol. wt. of S = 30.06 g) is added slowly to the hydrazine hydrate ($NH_2NH_3^+OH^-$). The solution of S/hydrazine thus obtained is placed in a bubbler connected to a tubular furnace. N_2 gas is passed through the bubbler into the furnace where the carbon material to be impregnated with S is placed. The systematic procedure for the synthesis of carbon materials from *Calotropis gigantea* and *Limonea acidissima* was provided elsewhere [21].

CHARACTERIZATION AND MEASUREMENTS

Electron Paramagnetic Resonance (Epr) Spectroscopic Studies

EPR spectra were recorded on a Varian E-112, X band spectrometer operating at a microwave frequency of 9.2 GHz and at room temperature using di phenyl picryl hydroxyl (DPPH) radical as the external reference to evaluate the g factor value and the spin concentrations. The experimental g-values were determined by substituting the measured values of H and ν into the following equation.

$$h\nu = g\beta H,$$

where h = Planck constant = 6.626×10^{-27} erg s,

β_e = Bohr Magneton of electron = 9.274×10^{-27} erg Gauss,

H = Magnetic field strength, in Gauss,
ν = Microwave frequency, in GHz,

From the EPR signal the number of unpaired electrons proportional to the area under the absorption curve, was deduced. The spin concentration was determined by comparing the area under the peak emerging from the known amount of the carbon sample with the area of the peak resulting from a known concentration of radicals from the standard, DPPH [23]. The spin concentration of paramagnetic centers in the carbon materials was calculated using Equation (1) [24, 25]:

$$N_x = \frac{A_x G_S M_S g_S^2 [\, S(S+1)_S \,] N_S}{A_S G_x M_x g_x^2 [\, S(S+1)_x]} \quad (1)$$

where the subscripts s and x represent the standard (DPPH) and the carbon material under evaluation (unknown), respectively.

A is the area measured under the absorption curve.
M is the modulation amplitude.
G is the relative gain of the signal amplifier.
S is the spin number.
g is the g factor of the EPR signal.
DPPH is used as a reference sample for spin concentration estimation.
The molecular weight of DPPH is 394.32 g/mol.
Therefore, the number of spins per mole of DPPH = 6.023×10^{23}.
That is, the number of spins per 394.32 g of DPPH contains 6.023×10^{23} spins.
Therefore, the number of spins per 1 g of DPPH = $6.023 \times 10^{23} / 394.32 = 1.527 \times 10^{21}$.

FT-IR Spectroscopic Studies

The FT-IR spectra of various samples were recorded on the Shimadzu spectrophotometer. The spectral range of analysis is 450–4000 cm^{-1} with a resolution of 4 cm^{-1}. The spectra were obtained in transmission mode at 20 scans. Pressed KBr pellets were prepared by grinding 200 mg of carbon samples with 0.5 g of KBr.

Scanning Electron Microscopy (SEM) with Energy-Dispersive X-Ray Analysis (EDXA)

SEM images of carbon materials were recorded using FEI QUANTA 200 FEG (field emission gun, virtual source) SEM equipped with an elemental analysis system. Carbon samples were placed on aluminum stubs using carbon tape and loaded into the microscope under ambient conditions. Care is ensured that the photographs recorded are representative of the whole of the material (sample) under study.

RESULTS AND DISCUSSION

The free electron concentration in the activated carbon materials is a measure of their electrical conductivity. The free electron concentration in activated carbon materials produced from biomass (Figure 2) and those of the commercial activated carbon materials (Figure 3) were deduced from the EPR spectra using DPPH as an external standard.

The g values of each of the signals seen in Figures 2 and 3 are close to that of the free electron g value (2.00232). As a result, each of the signals seen in the EPR spectra is attributed to unpaired electron spins. Such free electron concentration is a measure of electrical conductivity [26] and is reflected in the electrochemical performance of electrodes fabricated from such carbon materials when used in energy storage and conversion devices [5].

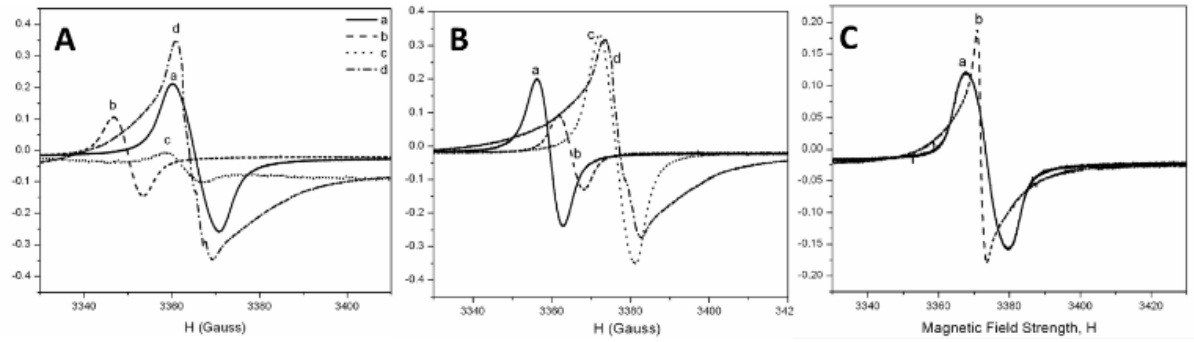

Figure 2. EPR spectra of carbon materials from (A) *Calotropis gigantea* [(a) char; (b) acid and base treated char, (c) char activated with K_2CO_3; (d) DPPH)], (B) *Ipomoea carnea* [(a) char; (b) acid and base treated char, (c) S functionalized activated carbon (current study); (d) DPPH)], and (C) *Limonea acidissima* [(a) activated carbon via KOH activation; (b) DPPH].

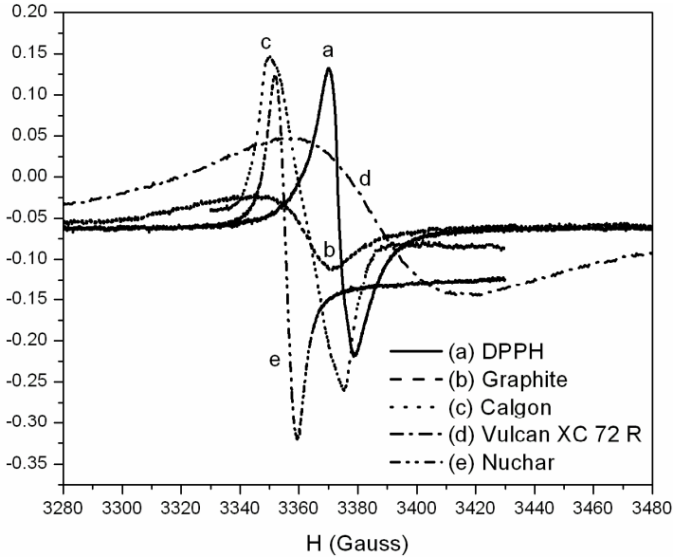

Figure 3. EPR spectra of (a) di phenyl picryl hydroxyl radical (DPPHP), external reference, and commercial activated carbon materials (b) Graphite (c) Calgon, (d) Vulcan XC 72 R, and (e) Nuchar.

As seen in Table 1, high spin concentration values observed in activated carbon materials from fossil-based sources, namely, acetylene black (0.38×10^{20}) and graphon black (0.11×10^{20}) could be derived from biomass-based carbon materials, like those produced from waste weeds *Ipomoea carnea* functionalized with heteroatom like S (0.983×10^{20}). Such heteroatom (S) containing carbon materials are potential cathodes for Li –S batteries [26, 27].

Important details from the data derived from the EPR spectra shown in Figure 2(A) and summarized in Table 1 about the paramagnetic centers in the carbon materials from *Calotropis gigantea* (Cg) were as follows: The g factor values of C_g as synthesized, Cg base acid and activated carbon from *Calotropis gigantea* are close to the g value of the free electron (2.002312) within the error of our experiments (± 0.002). The peak-to-peak separation was found to be higher in the case of biochar from *Calotropis gigantea* (ΔH = 11.0 Gauss) compared to either base acid or potassium carbonate-activated biochar. Such a broadness in the EPR signal is attributed to the presence of SiO_2 in the original char. The decrease in ΔH value upon treatment with base and acid indicates the removal of the silica. In addition, the broadness is contributed by structural changes as well. It is observed that upon activation with K_2CO_3, the ΔH value increased from 6.0 to 9.5 G due to the presence of traces of K in the carbon material after activation leading to the slight broadening in the EPR signal. The concentration of unpaired electrons in the biochar was found to be of the order of 0.73×10^{19}/g. The origin of such spins is attributed to the

generation of dangling bonds formed because of the extensive devolatilization from the defragmentation of the hemicellulose, cellulose, and lignin structure during the preparation of the char in the muffle furnace at 573 K. Paramagnetic centers were found to be associated with the dangling bonds formed during the carbonization of carbon materials. The spin concentration of the graphon black and acetylene black [28] were 1.1×10^{19} and 3.8×10^{19} spins/g respectively which are of the same order of magnitude as that of the spin concentration value observed in the case of the unactivated biochar. Upon treatment of the char with base and acid, the spin concentration decreased from 0.74×10^{19} to 0.34×10^{19} spins/g. Nearly a three orders of magnitude reduction in the spin concentration is observed upon activation of char with K_2CO_3 (0.15×10^{16} spins/g). Such a drastic decrease in spin concentration upon activation with K_2CO_3 is because of the saturation of the dangling bonds with K metal, formed during the carbothermal reduction of K_2CO_3, resulting in the formation of surface C–K bonds which subsequently transform to C–H bonds upon final treatment with conc. HCl. Such a transformation is also confirmed by the increase in the hydrogen content (2.63 to 3.5 wt.%) of the carbon sample activated with K_2CO_3 and subsequently treated with conc. HCl. For comparison the EPR spectra of some of the well-known commercial carbon materials, namely, Graphite, Calgon, Vulcan XC 72 R, and Nuchar were recorded and are shown in Figure 3. The g values as well as the spin concentration values were summarized in Table 1. The g values of commercial carbon materials were found to be close to that of the g value of free electrons (2.00232) whereas the spin concentration values of the commercial carbon samples were found to be two to three orders of magnitude higher than the value observed for activated carbon from *Calotropis gigantia*.

Table 1. Free electron concentration in activated carbon materials (biomass-derived vs. commercial).

Activated Carbon Material	**Free Electron Concentration (spins/g)**	**g-Value**
Biochar from *Calotropis gigantea*	0.73×10^{19}	2.00092
Biochar from *Calotropis gigantea* after treatment with base followed by acid	0.33×10^{19}	1.99980
Activated (K_2CO_3) carbon from *Calotropis gigantea**	0.15×10^{16}	2.00058
Biochar from *Ipomoea carnea*	0.575×10^{20}	1.99832
Activated carbon from *Ipomoea carnea* after base followed by acid treatment	0.239×10^{20}	1.99916
Activated carbon from *Ipomoea carnea* with S functionalization	0.983×10^{20}	2.00082
Activated carbon from *Limonea acidissima**	0.13×10^{19}	2.03095
Acetylene black[1]	0.38×10^{20}	–
Graphon black[1]	0.11×10^{20}	–
Graphite	0.14×10^{18}	2.01805
Calgon	0.23×10^{19}	2.00050
Vulcan XC72R	0.16×10^{19}	2.00839
Nuchar	0.53×10^{18}	2.01284

Note: DPPH – diphenyl picryl hydroxyl radical, the standard used in the EPR analysis for the quantification of free electron concentration in various commercial and biomass-based carbon materials (0.153×10^{22} spins/g); *data extracted from [21]; [1]data extracted from [29].

The presence of paramagnetic spins originating from the dangling bonds is evident from the signal emanating from the carbon materials [biochar, base (NaOH) and acid (HCl) and treated biochar and S functionalized activate carbon] from *Ipomoea carnea* as shown in Figure 2(B). The g values and the spin concentration values deduced from the EPR signals were summarized in Table 1. The g values were found to be close to that of a free electron g value (2.00232). Also, the spin concentration value was found to decrease upon treatment with acid and base which is a result of the saturation of dangling bonds. A four-fold enhancement in the spin concentration value is observed upon S functionalization of the acid and base-treated biochar sample from *Ipomoea carnea* is observed as evident from the increase in the intensity of the EPR signal relative to either as synthesized sample or the base and acid-treated carbon material (Figure 2(B)). It is a known fact in chemical literature that radicals are formed upon heating S. The diamagnetic S8 ring of S will be cleaved upon heating resulting in the formation of high molecular weight S_x chains possessing one unpaired electron at each end of the chain. As the

chains of S were very very long, the expected increase in the concentration of free electrons is not very high and so, only a four-fold enhancement of spin concentration is observed upon S functionalization (Table 1) [23]. Sulfur functionalization (0.34 wt. %) activated carbon material Ipomoea carnea was ascertained from SEM with EDX analysis (Figure 4).

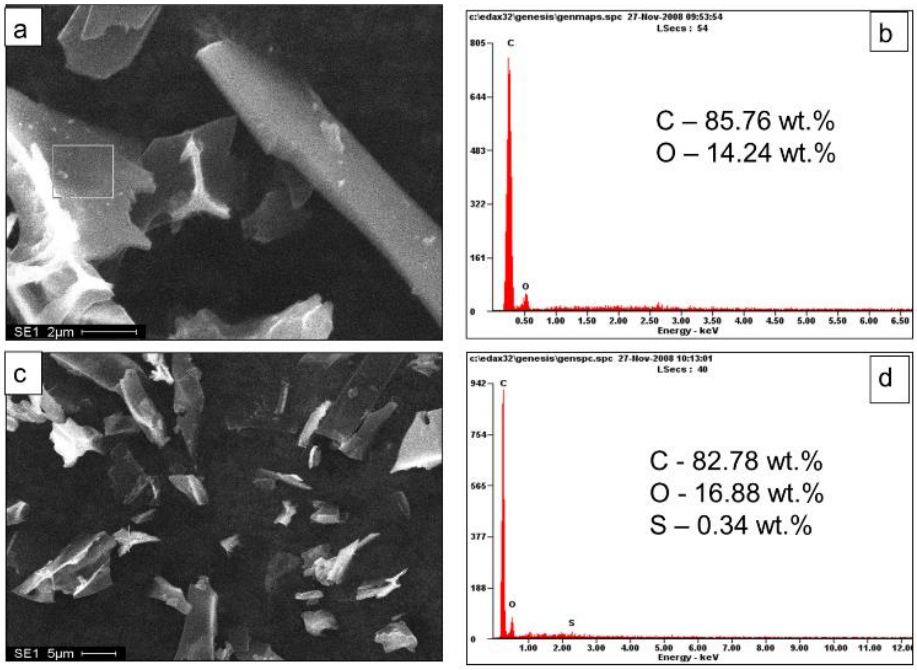

Figure 4. SEM images with EDXA spectra of (a, b)) base and acid-treated biochar from *Ipomoea carnea* and (c, d) sulfur functionalized activated carbon *Ipomoea carnea*.

Moreover, a band at 1165 cm^{-1} in the FT-IR spectra of S-functionalized activated carbon from *Ipomoea carnea* is characteristic of the presence of the C=S bond due to S functionalization (Figure 5). In addition, a shoulder at 1693 cm^{-1} is observed in the case of the S-functionalized carbon sample characteristic of C=O absorption in carboxylic acids. This shows the effectiveness of the chemical synthesis method in imparting S functionalization apart from the usual oxygen functionality upon activation.

In addition to high free electron concentration, the carbon materials derived from biomass possess many interesting physicochemical properties; like peculiar microstructure and porosity depending on the plant tissue architecture. The tenability of microtextural architecture, namely specific surface area and porosity in biomass-based carbon materials relative to commercial activated carbon materials produced from fossil-based resources is exemplified in the following figure.

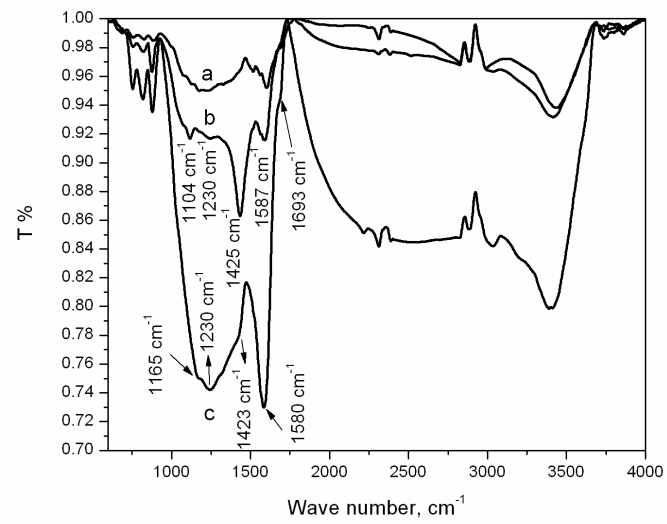

Figure 5. FT-IR spectra of carbon materials from *Ipomoea carnea* (a) biochar (b) biochar treated with a base and an acid in succession and (c) S functionalized activated carbon.

With the same biomass under different activating conditions (for instance the stems of *Calotropis gigantea* activated with $ZnCl_2$ and K_2CO_3 as two different activating agents), physicochemical properties of carbon materials can be varied drastically [21]. Such tailoring of free electron concentration and textural properties is not very flexible and diverse with fossil-based activated carbon materials. There are many more unique features of biomass-based carbon materials that make them indeed promising candidates for electrochemical device applications [30].

In Chemical communications, free electrons are synonymous with currency [29, 31–35]. The electrical conductivity of carbon material is intimately related to the free electron concentration [26]. Apart from its use in electrochemical energy sources, such free electrons play a crucial role in the degradation of environmental pollutants owing to their radical scavenging ability. Adolfsson and coworkers reported carbon nano-micro particles prepared from glucose, with and without hetero atom (nitrogen) using different solvents (water, ionic liquids) under microwave irradiation for 5 minutes at 180 °C. The free electron concentration of such carbon particles is nearly three orders of magnitude higher ($4–12 \times 10^{22}$ spins/g) [29] than those activated carbon materials shown in Table 1. This shows that with evolving synthetic strategies and biobased feedstock (like glucose), the free electron concentration can be varied over a wide range and the electrode performance of the carbon materials as a function of free electron concentration can be evaluated. In chemical literature, these free electrons in carbon structure were loosely called persistent free radicals (PFR) [29], dangling bonds, σ radicals [26], and paramagnetic defects [31, 33].

The origin of the EPR signal in carbon materials with a g-value centered around 2.00232 is still a matter of debate and systematic experimentation is needed [32]. However, we do agree with other pioneers in the field, that the origin of this paramagnetic resonance signal from carbon materials (observed in biobased and fossil-based) in high probability could be due to unpaired electron localized in a carbon dangling bond [32–34]. Jia et al., newly identified satellites to the main ESR signal originating from the thin diamond films. These satellites were attributed to the dangling bond – H centers which were suspected to be the bulk defects [34]. However, in none of the carbon materials shown in Table 1, such bulk defects were identified. Any information on the structure of the dangling bond – C centers is most wanted as of now.

Watanabe and Sugata surmised the appearance of the ESR central signal in the diamond thin films (with a spin density (Ns) of ~ 10^{18} cm^{-3}) to the large amount of carbon dangling bonds which were

orphaned after the delivery of hydrogen during the crystal growth process. However, the truth is not yet revealed [35].

CONCLUSIONS

Activated carbon materials from biomass deliver large amounts of carbon dangling bonds. Such huge amounts of free electrons (~1020 spins/g) equip them with enhanced electrical conductivity. This will have implications not only in the improvement of the performance of electrochemical energy sources but also in designing electron spin resonance imaging techniques as well as EPR-based oximetry used as clinical non-invasive in vivo probes for localized O2 concentration. Owing to the strategic application of the free electron concentration in carbon materials from biomass, it is necessary to probe the structure and dynamics of the carbon dangling bonds most often preferring the neighborhood of suspected dangling bond – H centers.

Acknowledgments

Gratefulness is due to Dr. Trupti Gajaria, the true physicist, for the idea of condensed matter physics. Indebtedness is due to Professor N Narasimha Murthy for teaching the course on EPR spectroscopy as part of the Ph D curriculum of INP at IIT Madras. Thanks are due to Mr. Siva Rama Krishnan, former in charge of the EPR measuring instrument for providing uncensored access. Indebtedness is due to Professor Ashok Kumar Mishra, former head of, the Sophisticated analytical instrumentation facility for the EPR facility. Professor Mahendra N Jadhav, librarian, central library, IIT Madras, and his efficient team are thanked for the uncensored access to the valuable resources that enabled the successful compilation of the manuscript. Thanks are due to the staff of the alumni association, IIT Madras for the access to the required facilities. Thanks are due to CRCL LLP caterers for the refreshing coffees and snacks. Thanks are due to the staff of the Campus café (Vajra caterers), IIT Madras for the food. Gratefulness is due to Mr Utkarsh Pathak, IIT Madras for installing MS Office on the laptop of INP enabling the successful compilation. Thanks are due to Mr. Aakash, Sunshine laptop service center for installing the solid-state drive and additional and accelerating the performance of the laptop of INP. Indebtedness is due to the Ms. Columbian Chemicals Company, USA for the generous funding. The generous funding and support of the DST, India to the National Center for Catalysis Research (NCCR), IIT Madras is acknowledged.

REFERENCES

1. Bandosz TJ. Exploring the silent aspect of carbon nanopores. Nanomaterials. 2021;11(1):407.
2. Ostrejko RV. Chemical activation of wood using $CaCl_2$. British Patent 14224. 1900.
3. Ostrejko RV. Process of producing decolorizing charcoal. US Patent US 1362064A. 1920.
4. Ostrejko RV. Process of obtaining carbon of great decolorizing power. US Patent 739104A. 1903.
5. Pulidindi IN. Development and exploitation of carbon materials from plant sources [Ph.D. thesis]. Chennai: IIT Madras; 2009.
6. Kumar YA, Mani G, Pallavolu M, et al. Facile synthesis of highly efficient construction of $WS_2/FeCo_2O_4$ nanocomposite grown on nickel foam as a battery-type energy material for electrochemical supercapacitors with superior performance. J Colloid Interface Sci. 2022;609:434–446.
7. Ghidin M, Lukatskaya MR, Zhao MQ, et al. Conductive two-dimensional titanium carbide clay with high volumetric capacitance. Nature. 2014;516:78–81.
8. Yao L, Lin JS, Yang HT, et al. Two-dimensional hierarchically porous carbon nanosheets for flexible aqueous supercapacitors with high volumetric capacitance. Nanoscale. 2019;11(1):11086–1192.
9. Zhou JS, Hou L, Lian J, et al. Nitrogen-doped highly dense but porous carbon microspheres with ultrahigh volumetric capacitance and rate capability for supercapacitors. J Mater Chem A. 2019;7(1):476–485.
10. Mao ZX, Wang CY, Shan QY, et al. Unusual low-surface area nitrogen-doped carbon for ultrahigh gravimetric and volumetric capacitances. J Mater Chem A. 2018;6(1):8868–8873.

11. Ding CF, Liu TY, Yang XD, et al. An ultra-microporous carbon material boosting integrated capacitance for cellulose-based supercapacitors. Nano Micro Lett. 2020;12(63):1–17.
12. Zhou JS, Lian J, Hou L, et al. Ultrahigh volumetric capacitance and cyclic stability of fluorine and nitrogen co-doped carbon microspheres. Nat Commun. 2015;6:1–8.
13. Pulidindi IN, Gedanken A. Can biofuels alleviate the energy and environmental crisis? New York: Nova Science Publishers, Inc.; 2019.
14. Sun L, Gong YN, Li DL, et al. Biomass-derived porous carbon materials: synthesis, designing, and applications for supercapacitors. Green Chem. 2022;24(1):3864–3894.
15. Lin Y, Li FF, Zhang Q, et al. Controllable preparation of green biochar-based high-performance supercapacitors. Ionics. 2022;28(1):2525–2561.
16. Zhou M, Yan SX, Wang Q, et al. Walnut septum-derived hierarchical porous carbon for ultra-high performance supercapacitors. Rare Met. 2022;41(7):2280–2291.
17. Yeletsky PM, Lebedeva MV, Yakovlev VA. Today's progress in the synthesis of porous carbon from biomass and their application for organic electrolyte and ionic liquid-based supercapacitors. J Energy Storage. 2022;80:1–28.
18. Jiang BX, Cao L, Yuan QH, et al. Biomass straw-derived carbon synthesized for supercapacitor by ball milling. Materials. 2022;15(1):1–11.
19. Tian N, Gao M, Liu XH, et al. Activated carbon derived from walnut green peel as an electrode material for high-performance supercapacitors. Biomass Convers Biorefinery. 2023;16781–1689.
20. Yue XE, Yang HX, Cao Y, et al. Nitrogen-doped cornstalk-based biomass porous carbon with uniform hierarchical pores for high-performance symmetric supercapacitors. J Mater Sci. 2022;57(1):3645–3661.
21. Viswanathan B, Pulidindi IN, Varadarajan TK. Development of carbon materials for energy and environmental applications. Catal Surv Asia. 2009;13(1):16483.
22. Victor A, Sharma P, Pulidindi IN, et al. Levulinic acid is a key strategic chemical from biomass. Catalysts. 2022;12(1):1–15.
23. Drago RS. Physical methods for chemists. Surfside: Scientific Publishers; 1992. 398.
24. Sarathi R, Rajesh Kumar P, Sahu RK. Analysis of surface degradation of epoxy nanocomposite due to tracking under AC and DC voltages. Polym Degrad Stab. 2007;92(1):560–68.
25. Wertz JE, Bolton JR. Electron spin resonance: elementary theory and practical application. 2nd ed. New York: McGraw-Hill; 1986.
26. Aumond T, Vezin H, Batonneau-Gene I, et al. Acidity: a key parameter in zeolite-templated carbon formation. Small. 2023;19(1):1–5.
27. Mishra R, Panda PS, Barman S. Synthesis of sulfur-doped porous carbon for supercapacitor and gas adsorption applications. Energy Res. 2022;46(1):2585–2600.
28. Donnet JB, Bansal R, Wang M. Carbon black – science and technology. 2nd ed. Boca Raton: CRC Press; 1993.
29. Adolfsson KH, Huang P, Golda-Cepa M, et al. Scavenging of DPPH by persistent free radicals in carbonized particles. Adv Sustain Syst. 2023;7(1):2200425.
30. Balasubramanian V, Pulidindi IN, Varadarajan TK. Preparation of activated carbon from a botanical source. Indian Patent No. IN200700376-I4. Indian Institute of Technology Madras.
31. Yan GP, Peng L, Jian SQ, et al. Bottle SE. Spin probes for electron paramagnetic resonance imaging. Chin Sci Bull. 2008;33(1):3777–3789.
32. Talbot-Ponsonby DF, Newton ME, Baker JM, et al. An electron paramagnetic resonance investigation of paramagnetic defects in diamond films grown by chemical vapor deposition. J Phys Condens Matter. 1996;8(1):837–849.
33. Fanciulli M, Moustakas TD. Defects in diamond thin films. Phys Rev B. 1993;48(1):14982–1588.
34. Jia H, Shinar J, Lang DP, et al. Nature of the native defects ESR and hydrogen dangling bond centers in thin diamond films. Phys Rev B. 1993;45(1):17595–17598.
35. Watanabe I, Sagata KJ. ESR in diamond thin films synthesized by microwave plasma chemical vapor deposition. Jpn J Appl Phys. 1988;27(1):1808–1811.

